The NOTCam Calibration Plan

Instrument, Detector, and Imaging Mode

A.A. Djupvik

December 11, 2006

Draft v.0.1.

Contents

1 Introduction 4

2 Detector characteristics 6
- 2.1 The Hawaii-I array . . . 6
- 2.2 Available readout modes . . . 6
- 2.3 Read noise and gain . . . 8
  - 2.3.1 Pick-up noise . . . 9
  - 2.3.2 Reset level drifts . . . 9
- 2.4 Darks . . . 11
  - 2.4.1 The dark images . . . 11
  - 2.4.2 The reset anomaly . . . 12
  - 2.4.3 Measured dark current . . . 13
- 2.5 Bad pixels . . . 14
  - 2.5.1 Hot pixels . . . 14
  - 2.5.2 Dead pixels and thermal cycles . . . 15
  - 2.5.3 Bad pixel treatment . . . 15
- 2.6 Linearity . . . 16
- 2.7 Memory effects . . . 17

3 Instrument characteristics 19
- 3.1 The cryostat . . . 19
  - 3.1.1 PTR vibration tests . . . 19
  - 3.1.2 Temperature stability of the detector . . . 19
  - 3.1.3 The vacuum . . . 20
  - 3.1.4 The problem with leaks during LN2 filling/spilling . . . 21
  - 3.1.5 The thermal cycle time . . . 21
  - 3.1.6 Temperature monitoring and warning systems . . . 22
  - 3.1.7 Maintenance and testing . . . 22
- 3.2 Mechanics . . . 22
  - 3.2.1 Bearings . . . 22
- 3.3 Optical quality . . . 23
  - 3.3.1 The optical design . . . 23
  - 3.3.2 The WF camera . . . 23
  - 3.3.3 The HR camera . . . 25
  - 3.3.4 Ghosts and stray light . . . 25
- 3.4 Focus . . . 26
  - 3.4.1 Internal camera focus . . . 26
  - 3.4.2 The focus pyramid . . . 27
- 3.5 Filters . . . 29

3.5.1 Transmission curves . . . 29
3.5.2 Narrow band filter vignetting . . . 29
3.6 Flat fields . . . 29
3.7 The shutter . . . 31
3.7.1 Initial problems . . . 31
3.7.2 Shutter accuracy . . . 32
3.8 Efficiency and throughput . . . 33
3.8.1 Choice of pass bands . . . 33
3.8.2 Accuracies and observational requirements . . . 34
3.8.3 Calculations of the zero points . . . 35
3.8.4 Photometric scatter over the FOV . . . 35
3.9 NOTCam overheads . . . 36

4 The NOTCam detector Quality Control 37
4.1 The already implemented detector QC . . . 37
4.2 Suggested upgrade . . . 38

5 The NOTCam imaging Quality Control 40
5.1 Twilight flats . . . 40
5.2 Photometric standard stars ($YnJHKs$) . . . 40
5.3 Data reduction . . . 41
5.3.1 Flat field images . . . 41
5.3.2 Standard star images . . . 43
5.3.3 Aperture photometry . . . 44
5.3.4 Data storage . . . 45

6 Tests upon mounting on the telescope 46

7 Annual tests 48
7.1 Vacuum cryostat health checks . . . 48
7.2 Focus pyramid . . . 48
7.3 Plate solution and optical distortion . . . 49
7.4 Shutter accuracy . . . 49
7.5 Memory effects . . . 49

A WF camera plate solution 51

1 Introduction

NOTCam arrived at the NOT in June 2001 after extensive testing by the instrument group at Copenhagen University Observatory (then called IJAF). At the NOT the instrument was under commissioning until the first visitor run started on 1 April 2002.

The purpose of the NOTCam Calibration Plan is to define how to make quality control of the data delivered by NOTCam. That is: how to monitor the performance of 1) the detector, and 2) the instrument (+ telescope) in imaging mode. (Quality control of NOTCam spectroscopy is not included here.) The idea of this document is to determine the content of the NOTCam quality control, e.g. what should be monitored, and how frequently, and how should this be implemented in practice.

The goal is to efficiently control long term effects, as well as promptly discover sudden problems in all three systems. The calibration data taken is at this point not intended to serve the community with calibrations to be used for data reduction purposes. Although the monitoring results and parts of the database output (e.g. badpixel masks, master flats, zeropoints etc.) may be interesting and useful when reducing NOTCam data (i.e. they should be available on-line), we strongly urge all observers to make sure they take their own calibration data of sufficient quality for their respective science projects if possible.

In Sections 2 and 3 the characteristics of the detector and the instrument are described. This is based on the experience obtained with NOTCam up to now and is used as a background for the selection of quantities that should be measured and monitored for health check purposes.

In practice, the Quality Control (QC) tests are divided into day-time tests and night-time tests. Therefore we suggest the two main quality control projects:

- **NOTCam detector QC** (see Sect. 4)
- **NOTCam imaging QC** (seeSect. 5),

where the first (already implemented in 2003) is performed day-time as soon as NOTCam has been mounted on the telescope, and the second one is intended for NOTCam technical nights with photometric/clear weather. Another set of tests are the:

- **NOTCam first night tests** (see Sect. 6),

which are performance tests that should be made the first day/night that NOTCam has been mounted on the telescope. The detector QC is one of these, and furthermore they involve centering of optical elements if needed (filters and stops), finding pinhole positions on the array, finding the rotation centre on the array, finding the alignment of the array with respect to the sky, and possibly slit alignment (on the sky) if the alignment has changed.

Quantities that are expected to be stable need to be checked only about once per year, or whenever there is a suspected problem. These tests are the:

- **NOTCam other tests** (see Sect. 7),

The **detector QC** has been running already since 2003. Here its content is documented, and we also suggest some upgrades (see Sect. 4).

2 Detector characteristics

2.1 The Hawaii-I array

The NOTCam detector is a Hawaii 1024 × 1024 HgCdTe array from Rockwell with 18.5 μm pixel size. The expectance value for well depth is 120 000 e^-, and the read noise is specified to around 10 e^- (although 3 e^- could be reached with multiple non-destructive sampling). The QE is expected to be around 60-70%, and the dark current is expected to be less than 0.1 e^-/s/pix. These are expected values. We will give examples in this text from the two arrays we have used with NOTCam: the Engineering Grade Array (P/N: 8-344R#1 #131) and the first Science Array (P/N: 9-173L A2 #61), also referred to as SWIR1 and SWIR2 locally at the NOT.

The detector is a hybrid structure consisting of an IR sensor made of HgCdTe which is "sandwiched" to a silicon readout multiplexer. The two arrays are bonded together pixel by pixel with indium bumps, which have high resistance to low temperature. The fact that photon detection and registering is made by two different arrays makes non-destructive readout possible, contrary to CCDs, where the same array both detects and reads.

The multiplexer is structured in four independent quadrants (see Fig. 1), each of which contains two digital shift registers for pixel addressing: one horizontal and one vertical. Each quadrant is thus read out sequentially using CMOS shift registers, and all four quadrants are read simultaneously. The reset is done line by line. Several bias voltages are applied, of which two are adjustable and determine the reset level of the pixel as well as the dynamical range. As charge accumulates in a pixel, the signal voltage decreases. The multiplexer reads the signal voltages of each pixel both before and after the integration. The output voltages are transmitted to four identical preamplifier channels before feeding this into four identical A/D converters.

The Hawaii-I array is operated by a Copenhagen University Observatory Controller. The readout time for 1024 × 1024 pixels is 3.6 seconds. With two readouts per exposure this corresponds to 7.2 seconds overhead to readout per exposure.

The internal power supply of the controller generated some noise which was picked up by the system producing a stripy interference pattern in the images. This pick-up noise was practically removed mid-2003 by making the physical distance between the power supply and the controller electronics larger.

2.2 Available readout modes

The NOTCam data acquisition software **NOTCam BIAS** (Klougart 2006) offers two readout modes: reset-read-read (also called Fowler sampling) and ramp-sampling. The reset-read-read mode works as follows: at the start of an integration

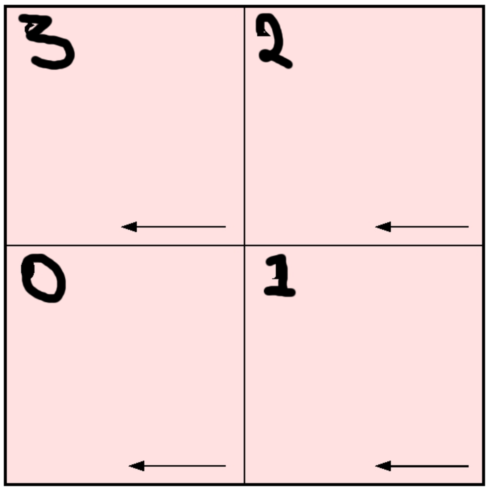

Figure 1: *The quadrant layout with fast readout direction and NOTCam numbering indicated. Note that this figure shows the situation since Jan-2006 when an X-flip was introduced. See Table 3 for a translation to Rockwell numbering or MEF header numbering.*

each pixel voltage is reset, and the array is read out to produce the *reset image*, also called the "pre" read. Then the shutter opens, the integration starts, the shutter closes, and the array is read again, producing the *end-of-integration image*, also called the "post" read. The *reset image* is subtracted from the *end-of-integration image* in order to obtain the result of the integration.

The ramp-sampling mode works as follows: the shutter is opened, then each pixel voltage is reset and read out to produce a *reset image* (takes 3.6 sec), during the exposure the array is read out the requested number of times at the requested interval, and after the last readout the shutter is closed. Then a linear regression analysis is made through all the readouts (including the *reset image*) to produce an additional image which is stored as the first of the image extensions in the FITS file. The linear regression analysis reduces the readnoise by a factor of $1/\sqrt{N}$ where N is the number of readouts used, provided the readout noise ifself is dominated by white noise. It is superiour to the reset-read-read mode in readnoise limited conditions. For this mode the exposure time is defined by the readouts and not by the shutter.

For each exposure mode **exp, mexp** and **frame** is associated a corresponding dark command **dark, mdark** and **dframe**. For more detailed information on both modes see Klougart (2006) for technical information and the online NOTCam User's Guide for practical use of the modes.

Table 1: *The two readout modes with NOTCam.*

Readout mode	Exposure command	EXPTIME	Data MEF file
reset-read-read	**exp t**	t	[1024,1024,2]
	mexp t N	t	N× [1024,1024,2] + [1024,1024]
ramp-sampling	**frame t N**	t×N	[1024,1024,N+2]

2.3 Read noise and gain

The readnoise should be around 10e$^-$ according to specifications. This is also the value measured for the Engineering Grade Array since 2003 (after removing the pick-up noise, see below). We lately (2006) measure a readnoise of 9.7±0.4 e$^-$ and a gain of 2.76±0.06 e$^-$/adu, averaged over all quadrants for the reset-read-read mode. The standard deviation given here is the spread between quadrants which is much larger than the temporal variation of each quadrant (in the periods of a well-behaving detector). We have used pairs of 0.5 or 1 sec dark images and well exposed dome flats and calculated the readnoise and gain according to Janesick's method for a number of small areas (to avoid bad pixels), of which a mean result per quadrant is extracted to the Detector QC database.

Table 2: *Typical values of readnoise and gain for the Engineering Grade Array in 2006. The sigma gives the spread between quadrants.*

Readout mode	Read noise (e$^-$)	Gain (e$^-$/adu)
reset-read-read	9.7±0.4	2.76±0.06
ramp-sampling	11±1	3.1±0.1

For the ramp-sampling mode the effective readnoise level is expected to be lower by a factor of $1/\sqrt{N}$ where N is the number of readouts. To actually measure the effective readnoise one must use the image which is the result of the linear regression analysis. Thus, in order to test for N=3 or N=10 we have to use rather long darks of 11-36 seconds. We find that the difference image of two 42 sec darks with N=10 gives a readnoise of around 10e$^-$, i.e. only marginal improvement. An alternative method is to look at the deviations from the linear fit made by NOTCam BIAS when applying the linear regression analysis to calculate a final frame. Both of these methods are complicated by the fact that the darks are not linear (see Sect. 2.4 and the on-line QC results on the www).

Our current readnoise and gain measurements for the ramp-sampling mode using

Janesick's method are made on the first 4.2s readouts of dark images taken with the **dframe** command, and the final regression analysis image of the raw dome flat obtained with the **frame** command. The average values and the scatter between quadrants are given in Table 2.

From the *Detector QC* database we can see that during the period with pick-up noise the average readnoise level was substantially higher while the gain was stable. During the problems with the reset level drifts (see Sect. 2.3.2) both the readnoise and the gain varied significantly. The readnoise and the gain should be frequently monitored for both readout modes. Each quadrant must be measured independently. These quantities should be monitored at the start of every NOTCam run.

2.3.1 Pick-up noise

From the arrival of NOTCam to the NOT in June 2001 some pick-up noise was always present in the images, but to a variable extent. As seen in Fig. 2 the effect was strongest in the two upper quadrants, and could amount to 20 ADUs peak-to-peak in low background images (such as darks). It was recommended to use the ramp-sampling mode with many readouts, to select integration times such that the background was around 1200 ADUs as a minimum, and to have at least 10-20 images to median combine in order to overcome this noise in the resulting images.

As a consequence of the pick-up noise combined with the fact that the data is stored as unsigned integers, there were frequently pixels which got negative values in the reset frame subtraction of very low count level images (e.g. darks). These negative values then wrapped around to very high positive numbers giving very noisy dark images. Before using such darks for anything all values above 60000 adu had to be set to zero.

The origin of the pick-up noise was finally found in mid-2003 to be the power supply of the detector electronics. Moving the power supply unit physically out from the electronics box by a few centimeters cured the problem. The readnoise diminished from 24 and 15 e^- in the upper and lower quadrants, respectively, to the specification value of about 10 e^-.

2.3.2 Reset level drifts

By "reset level" is here meant the count level in the so-called *reset image*, i.e. the image which is read out immediately upon resetting the capacitor and before the integration starts. The reset level can be adjusted by changing some array voltages from within the NOTCam data aquisition software. Typical values for our Engineering Grade Array are given in the script below. The first line sets the gain to *high*, which is the default for NOTCam. The next four lines set the "reset voltage" (Vrst) to 0.55 V for all four quadrants. This is the reset voltage that is applied to the array during the reset operation. The four last lines are the "biasgate" voltages

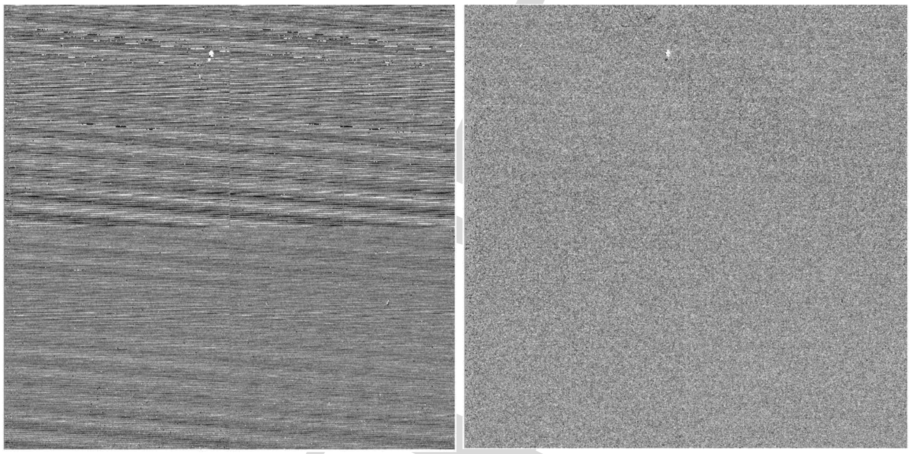

Figure 2: *Illustration of the pick-up noise present (left) and gone (right). Both images are difference images of two independent dark images.*

which vary a little from quadrant to quadrant, but are around 3 V. These are the ones that may need adjustment if the reset level starts to drift.

Note that the quadrant numbering from 0 to 3 in the script below is the NOTCam numbering convention as described in the web page:
www.not.iac.es/instruments/notcam/eng-grade-arr.html and as marked on the pre-amplifiers on the instrument. This numbering convention is different from both the one used by Rockwell, and the one in the image headers of the stored multi-extension fits files (MEF format introduced Jan-2006). See table 3 for a translation between them. Why a different scheme than Rockwell numbering was used for NOTCam is not known, but the reason for the differences in the MEF header keywords is that the MEF format per definition sets quadrant [1:512,1:512] to be quadrant one, quadrant [513:1024,1:512] to be quadrant two, etc. In addition, a flip in x-axis was done with the introduction of the MEF format to comply with standard orientations.

Table 3: *The various numbering conventions of the quadrants.*

NOTCam	Rockwell	MEF header
0	1	1
1	2	2
2	3	4
3	4	3

The below script is called *volt_eng* and works well for the Engineering Grade Array at the time of writing (May-06). The Science Grade Array used values found in the script *levelscience*. As soon as the voltages are established, the corresponding script is run automatically upon starting the data aquisition software. The values of the voltages are determined by finding a reasonable reset level and adjusting each quadrant to obtain the same overall level. A "reasonable" reset level is one which is high enough to minimize the number of zero pixels, but low enough to maximize the range of the linear regime. In October 2005 upon the installation of the Science Array a level around 5000-6000 ADUs was selected.

In the period Sep-2003 to May-2005 the reset level of the engineering grade array gradually decreased from an initial value of around 4000 ADUs (checked during commissioning in 2001) to an average value close to zero. This produced a gradual increase of zero pixels, and up to 30% of the array gave zero valued pixels at some point. Adjusting the BIAS voltages recovered the original reset level and the percentage of zero pixels decreased to around 1%. The reason for this drift of the reset level is not understood but it is probably inherent to the array. This previous experience with the engingeering grade array shows the importance of always storing the reset images and strongly suggests that the reset level must be monitored frequently, preferrably every time NOTCam is mounted for a new run.

```
@MODE0
@VBLA00+00550
@VBLA01+00550
@VBLA02+00550
@VBLA03+00550
@VBGX00+03120
@VBGX01+02910
@VBGX02+03115
@VBGX03+03120
```

2.4 Darks

Dark integrations are obtained with the commands **dark, mdark** and **dframe**. The latter was introduced to NOTCam BIAS in 2002 to allow for dark current measurements using the ramp-sampling readout mode.

2.4.1 The dark images

The appearance of the NOTCam dark images are shown in Fig. 3 for both the Engingeering Grade Array (top) and the Science Array (bottom) for zero exposures and longer (50-100s) exposures. The amplifier glow is clearly visible for the longer darks, as well as an increased number of hot pixels. The amplifier glow subtracts

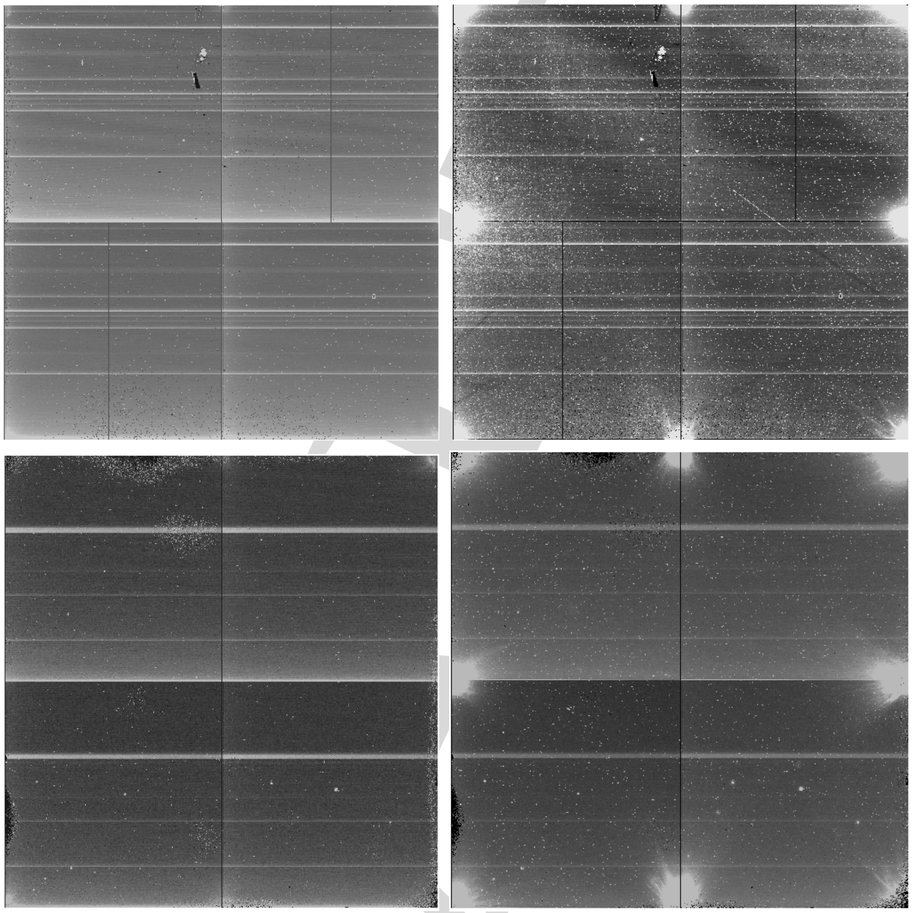

Figure 3: *Dark images of 0 seconds (left) and 50-100 seconds (right) exposure time for the Engineering Grade Array (top) and the Science Array (bottom).*

out well. The hot rows, located on the same place in each quadrant, are stable and subtract out well. They are probably intrinsic to the arrays.

2.4.2 The reset anomaly

The first rows that are read out in each quadrant have a higher intensity than rest of the quadrant. See the image and vertical cut in Fig. **??**. This intensity ramp at each quadrant is called the reset anomaly and is an additive effect. All IR detectors suffer to some extent from this effect. It is described technically by Mackay (1999).

Usually, the effect subtracts out quite well using sky subtraction as long as the intensity level has stabilized. Therefore, if the observations consist of few dithered frames only, it may be a good idea to skip the first image in the dithering sequence before shifting and median combining. It may also be recommended to add a fiducial

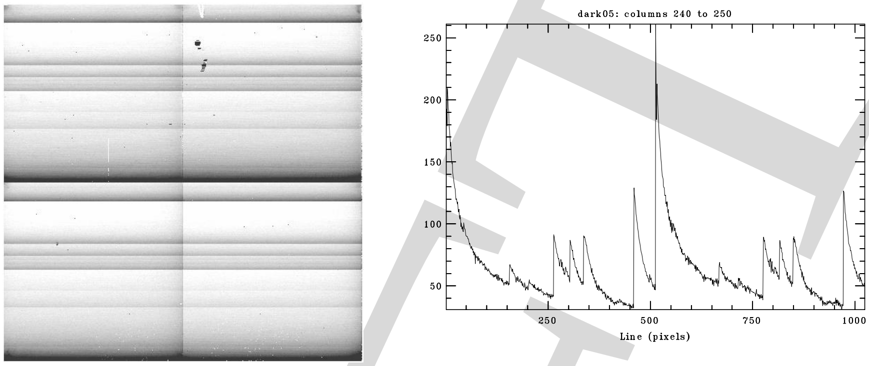

Figure 4: *Inverted image of 5 median-combined 0.5s darks and a vertical cut shows the higher intensity at the bottom of each quadrant where the readout starts. Also, the profile shows how the hot lines decay gradually. The median level over the image is 57 ADUs.*

first dither, which is later thrown away, only to let the detector stabilize first. When the detector has stabilized the ramp subtracts out well.

With WFCAM/UKIRT it is found that the ramp is stable for a given set of exposure modes and that master darks can be used to correct for it. With NOTCam we do not recommend this because of the issue with the darks described below.

2.4.3 Measured dark current

The measured dark current is non-linear, variable and higher than the specifications value of < 0.1 e^-/s/pix. Figure 5 shows a typical result obtained from the *Detector QC* for the reset-read-read mode. The dark current is measured at a level of ~ 1 ADU/s/pix (2.8 e^-/s/pix) for dark images of 30 seconds, but is substantially higher for shorter integration times: ~ 16 e^-/s/pix for 12 sec and ~ 140 e^-/s/pix for 1 sec. From the QC we know that this behaviour, although unexpected, is quite repetitive. The darks are taken in the following order (of integration times): 0.5, 42, 2, 30, 12, 18, 24, 36, and 1 seconds. They are a multiple of 5 (using **mdark t 5**) to avoid spurious jumps, and they are taken just before domeflat exposures of the same integration time. Before each multiple dark is started, the array is cleared twice.

Sudden jumps in the dark level have also been seen. As an example, the dark level was roughly constant at 80-100 ADU for a number of darks with exptimes between 0.2 and 10 seconds and then suddenly jumped to 260 ADU for one 0.8 sec exposure.

The reason for the strangely behaving darks is believed to be found in the electronics, as there are a couple of voltages missing (the 3.5V BIASGATE voltage and

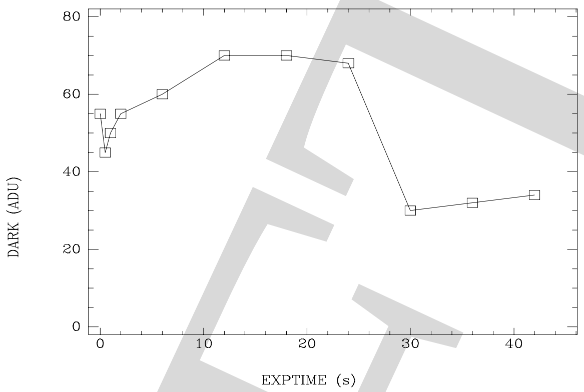

Figure 5: *The typical behaviour of the dark current measured in the* Detector QC *monitoring.*

BIASPWD voltage) compared to the standard configuration of these arrays. Until the behaviour of the darks is properly understood or the electronics are upgraded, we recommend users to avoid making separate dark subtraction, especially if the darks are taken at another time than the science images. Since sky subtraction is always needed in the IR, the dark is automatically subtracted out with it.

The darks should be regularly monitored.

2.5 Bad pixels

Bad pixels are pixels which are useless because they are dead or deviate strongly in response. We distinguish between hot, cold, and zero pixels. A zero pixel is not necessarily a dead pixel. A hot/cold pixel is a pixel whose value deviates from the mean level by more than $\pm$ 8 σ. A good IR array is an array with less than 1 % bad pixels. Both the engineering and the science grade arrays had in total $\sim$ 2 % bad pixels (calculated for 42 sec dark exposures) – mainly along the edges in the case of the science array.

2.5.1 Hot pixels

The amount of hot pixels increases with the integration time. See Fig. 6 which shows the behaviour of the central 250 $\times$ 250 pixels in the top left quadrant (Q3) of the science array for single dark exposures. It is seen that the effect is around 1% for the typical exposure times used in imaging mode ($\sim$ 100s). Hot pixels may also be strongly non-linear. In 42 seconds long darks there are on the average 1.4% hot pixels (over the whole array) while in well illuminated 42 second long exposures there are $<$ 0.2%.

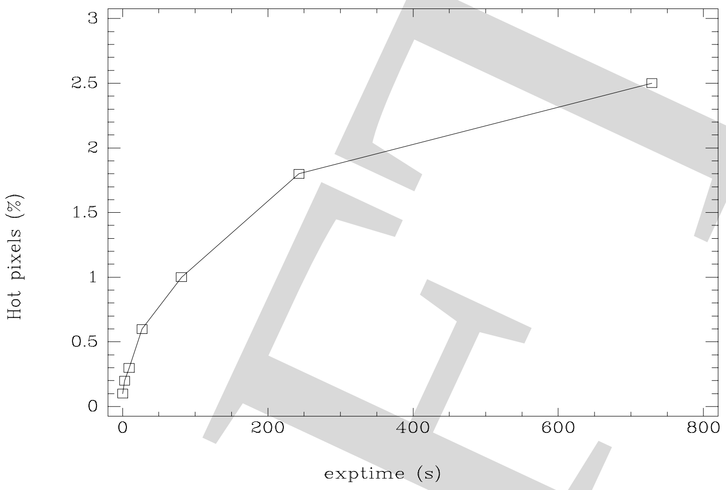

Figure 6: *The percentage of hot pixels increasing with exptime. Measured in the central 250×250 pixels of the top-left quadrant (Q3) on dark images.*

2.5.2 Dead pixels and thermal cycles

The number of dead pixels is generally believed to increase with every thermal cycle of the array. This is because of the different thermal expansion properties of the layers of an infrared array, which may cause detachment of the indium bump bonds upon repeated thermal cycles. This is also the reason why an engineering grade array is provided for the commissioning/testing when a science grade array is purchased. The NOTCam engineering grade array has undergone a number of thermal cycles during the more than 4 years it has been inside NOTCam. We have not seen any long-term increase in the number of zero-level pixels. The apparent coming (and going!) of "dead" pixels was found to be due to a drift in the array causing the reset level to vary. This effect is described in Sect. 2.3.2. Since then we call zero level pixels simply "zero" pixels and not "dead" pixels. Nevertheless, it is still recommended that the number of thermal cycles is kept to a minimum. Monitoring the percentage of zero pixels is still necessary. Among the zero pixels are included the two dead columns at x=1 and x=513 which are features of the controller configuration.

2.5.3 Bad pixel treatment

For imaging purposes the bad pixels are best handled by filtering them away using the repeated, random ditherings of the telescope (which are normally always made) to subsequently shift the images and combine the images using a median. A badpixel mask can be used to flag the bad pixels in any image combination routine, which is recommended whenever the number of combined images is not abundant. It is generally not highly recommended to interpolate over bad pixels with neighbouring values if this can be avoided.

For spectroscopy it is important to keep track of possible useless positions on the array, for instance clusters of hot pixels. It was noted that the science array had some clusters of hot pixels not seen to the same extent in the engineering grade array. Their location strongly limits the positioning of a star on the slit. Usually the star is dithered along the slit on two positions in the frequently used ABBA pattern mode. Bad pixels cannot be filtered out as effectively as for imaging. IRAF tasks originally developed for cosmic ray removal can be very useful. Also, interpolation over bad pixels with neighbouring values is often done.

Not only the percentage of bad pixels (which is the quantity we have monitored in the *Detector QC* up to now) but also their location should be found and archived. The bad pixel result from the *Detector QC* should be stored as a bad pixel image with a number coding for the type of bad pixel (hot, cold, zero). The bad pixel mask should be stored in an archive, and can be of use to the observers (for instance ToO data), although bad pixel masks can easily be made per observing run by taking a set of darks. Currently only the percentage of cold, hot, and zero pixels is stored in the detector QC database. A JPG image shows the location of the bad pixels for the most recent QC results on the qc web page. This should be upgraded to the archival of one badpixel mask in fits format every time the *Detector QC* is run.

2.6 Linearity

Non-linearity between photon flux and output voltage is an inherent problem for IR arrays. Unlike for optical CCDs, the detector capacitance is not fixed, but depends on the reverse bias voltage, which itself changes continuously during integration. In principle, the non-linearity of an array can be calculated (McLean 1997) as it depends on parameters like doping concentrations and dielectric constants of the material, values which can be obtained from the manufacturers. An IR array is considered good in terms of linearity if this is better than 1% over 80% of the full-well depth.

For practical purposes it is necessary to know the dynamical range within which the detector is linear to within a given limit. This can easily be tested by a number of dome flats of different exposure times. For most purposes, it is sufficient to know the countlevel (in ADUs) where the detector starts to deviate more than 1% from linearity, to prepare one's observations such that the data is within this range. It is not known how stable the linear range is. This limit should therefore be monitored. Each quadrant must be tested invididually. The test should be made as frequently as at the start of every NOTCam run. It is vital to have a constant brightness lamp for this.

At the moment we are using a normal bulb in the dome. This should be considered improved for the future. We cannot guarantee that bulb brightness instability does not affect the data, but we use repeated measurements with both readout modes. For the reset-read-read mode the data is obtained with exposure times in the order: 0.5, 42, 2, 30, 12, 18, 24, 6, 36, and 1 second, interspersed with equally long darks, in order to diminsh long-term brightness variations. For the ramp-sampling mode eight different exposure commands of type **frame 4.2 10** are used, each of them giving a linearity test in the range from 4.2 to 42 seconds exposures. The results are always more reliable for the ramp-sampling mode, which is understandable as the whole dynamical range is tested within 50 seconds and this is repeated eight times. This mode does not sample the shortest exposures and the lowest light levels, however. In general, it is found that the Engineering Grade Array has a useful linear range (to better than 1%) up to $\sim$ 16000 ADUs or more. The Science Array has a linear range up to $\sim$ 27000 ADUs or more. There are some small long-term variations in these limits, but it is unclear if this is dominated by measurement and analysis errors. The deviations from linearity seen in the QC plots for the shortest exposure times (0.5, 1, and 2 seconds) are related to the shutter, see Sect. 3.7.

With more accurate calibration data, the correction for the non-linearity should be calculated and made available to the user-community in terms of the coefficients A, B, C in the relation

$$I_{\mathrm{corr}} = A \times I_{\mathrm{obs}} + B \times I_{\mathrm{obs}}^2 + C \times I_{\mathrm{obs}}^3 \tag{1}$$

as well as a goodness of fit indication. The ISAAC/VLT solution is to produce a template image for each coefficient to account for pixel to pixel effects. For NOTCam this should be looked more into in the future.

2.7 Memory effects

Another problem with IR arrays, not present in modern CCDs, is the persistency problem, also called the "memory" effect. This consists in each pixel having a memory of the light level it has experienced earlier. Luckily, this effect is relatively small in Hawaii-I arrays and it is not necessary to look at the whole time history of each pixel in order to correct its response. Nevertheless, the effect is far from negligible, and special precaution must be taken. The effect varies from array to array.

In normal conditions, when the array is not saturated (i.e. the signal $<$ 40000 ADU for the engineering grade array), the memory effect manifests itself as a *negative* ghost signal of magnitude $<$ 1% in the first subsequent read only, and then disappears. A pixel which has had level of 10000 ADUs will have 100 ADUs negative on the next read. In background limited conditions these errors of the order of 1%

or less in individual images are usually smoothed out to even smaller errors with the number of shifts and adds. If the subsequent image is one of a very low background (spectrum or dark), however, the negative memory may reach zero or even negative values. In this case there will be a wrap-around effect of negative values onto large positive counts (> 60000) because the images are stored as unsigned integers. The wrap-around effect of this "negative saturation" makes the images look very noisy.

Saturated pixels produce more nasty memory effects than non-saturated pixels. The first subsequent readout has again a *negative* ghost signal of magnitude $\sim 1\%$. The reason for the negative ghost is probably a transient lowering of the gain. The second readout has a *positive* ghost of magnitude 0.2%. Positive ghosts continue on several readouts. On the 6th readout its magnitude is 0.03%. The brightness of the ghost keeps decreasing with the number of reads, but since they are present for a while they will not be entirely removed by median filtering.

Saturation should be avoided as far as possible. The new clean-array BIAS command **clear**, introduced in the upgraded version from 2006, does a reset and a single read without storage, nor autoshow, and takes only 3.5 seconds. Repeated use of this command in between saturated images is highly recommended in order to minimize memory effects.

3 Instrument characteristics

This section describes characteristics not inherent to the detector itself but to the instrument in general (or the combined effect of the instrument and the telescope). A first presentation of NOTCam was given in Abbott et al. (2000).

3.1 The cryostat

The NOTCam vacuum cryostat is a cube with sides of 60cm . A document on the vacuum behaviour of NOTCam and recommendations for operation was made by Sørensen (2000). The cold table, which is vertical when the instrument is in use, is in contact with a $40 \times 40 \times 10$cm LN2 tank. The tank takes 16 l and has one fill tube and one vent tube. In addition, a vibration-free *Pulse Tube Refrigerator* (PTR) called CryoMini from Iwatani is used to reach an operating temperature of -199 degrees C (74 K) at the location of the detector. The cold table is mounted on fibreglass legs and surrounded by a radiation shield. Both the shield and the bottom of the cold table are wrapped in a superinsulating blanket. The vacuum is maintained by a charcoal getter.

3.1.1 PTR vibration tests

We detect no vibrations in the images taken in good seeing conditions (fwhm $\sim$ 0.5") – i.e. measurements of stars with the PTR on and off are indistinguishable.

3.1.2 Temperature stability of the detector

Typically, the temperature of the array during observations is stable to ± 0.1 degree[1], unless there has been substantial spilling through the vent tube. During commissioning spilling was found to be worst at rotator positions -20 to -80. The best field orientation of NOTCam with regards to spilling was determined to be **field-r -90** for normal observing. It was also recommended not to observe lower than 30 degrees altitude. Spilling of LN2 was problematic as it caused the detector temperature to rise. (Until January 2003 the PTR could not be used when NOTCam was mounted on the telescope because the long flexible hoses needed for He transport between the cold head and the compressor had not yet arrived.) Another problem with spilling was that it caused small vacuum leaks. These problems are now solved, and LN2 spilling is not critical. The default field orientation for NOTCam is still set to **field-r -90**, but this can be modified and has to when for example doing spectroscopy on the parallactic angle. Also, observations can be made at altitudes down to the limit of the telescope at 6.4 degrees.

[1] This is the temperature measured by the sensor mounted on the back of the detector flange.

3.1.3 The vacuum

The vacuum obtained at the NOT has never been as good as the one obtained in the lab at CUO (typically 3 $\times 10^{-6}$mbar the first day cold and improving with time). The best vacuum ever reached at the NOT is 2 $\times 10^{-5}$mbar when cold. It is not clear whether this is due to outgassing of components installed or small vacuum leaks.

After every closing of NOTCam, pumping is going on for at least two days before cooling is started, and usually a vacuum of 1 $\times 10^{-3}$ mbar is reached within 48 hours of pumping. The pressure normally goes down to 3 $\times 10^{-5}$ mbar when the instrument has reached operating temperature.

According to (Sørensen 2000) the getter needs to be baked if the pressure is higher than 1 $\times 10^{-4}$ mbar when NOTCam is cold. Such a bad vacuum means that either there is some leak or the getter has saturated.

Some experiences with the vacuum are listed:

- In order to increase the vacuum pumping efficiency we changed valve and hose diameters from 25 mm to 40 mm, but no improvement was seen in the obtained vacuum.

- Various leak tests have been performed using the Residual Gas Analyzer (RGA). Only negligible micro-leaks were found close to one of the preamplifier connectors.

- We have noted occurences of the Balzer pressure sensor showing unreliable values. No improvement in behaviour after cleaning the sensor.

- Care has been taken to keep the croystat clean. A special vacuum cleaner was purchased for the use in the clean room only. Metallic components are cleaned with acetone. The o-rings are cleaned with alcohol only.

- It has been found to be vital that the pumping is started within 15 minutes upon installing the newly baked charcoal while the getter is still hot. Therefore the mounting of the getter on the cold table has been simplified to allow quicker closing. This also means that it is not recommended to do a proper leak test upon every closing, simply because the valuable time while the getter is hot gets lost and pumping will be started too late.

- The charcoal for the getter has been replaced with new charcoal a number of times without any obvious improvement of the vacuum.

- The whole getter (without the paper filter and the lid) is to be baked in an especially purchased owen in the clean room at $\sim$ 140 degrees for a couple of days.

- If the cause of the problem is not found, there will be a frequent need to bake the getter in the future. Currently, this means the transport of NOTCam to and from the service building, a time-consuming procedure which also involves some risks. A simpler solution for baking and installing the getter (without having to open NOTCam in the traditional way) is currently looked at.

3.1.4 The problem with leaks during LN2 filling/spilling

This specific problem was recently solved and refers to vacuum leaks during filling and spilling of LN2 through fill and vent tubes. The problem initiated with the reduced LN2 filling time (from 1 hour to 5 min) in Mar-2002 when we started using a much wider filling nozzle which was fixed by a cap around the filling tube of NOTCam. Looking backwards in time this is now clear, but because observations were normally not performed at low altitudes, and because the effect would depend on rotator angle, the leaks were not immediately connected to the spilling of LN2. Also, the leaks when filling with LN2 varied from time to time, probably related to spilling of the nozzle itself. By the end of 2005, however, the problem was fully understood. It was caused by temperature stresses in the fill and vent tubes and deformation of o-rings causing minor but repeated vacuum leaks. Then the following changes were made:

- During observations the fill tube is blocked to minimize spilling and protect items below it. Previously, the blocking was done with a piece of foam rubber. Now the blocking is made with a special cork made of a superinsulating material. The cork is only in contact with the inner tube.
- Ventilation and spilling is allowed through the vent tube which is metallic and extended all the way to the bottom of the instrument in order to protect the surroundings from LN2.
- Both the fill and vent tube are protected thermally with heating tape around the most sensitive parts to avoid accumulation of ice, thermal stresses, and deformation of o-rings.
- Instead of being a cap going around the fill tube, the filling nozzle is now going inside the fill tube, being in contact with the inner tube only. It goes in only a very short distance to not damage the sensitive parts further in. (Perhaps the nozzle should be somewhat longer to avoid that the largest flux of LN2 flushes around the o-rings.)

3.1.5 The thermal cycle time

One thermal cycle of NOTCam including the transport to and from the service building takes in practice around 10 days. The warm-up time can be as quick as 3 days from the moment the PTR is turned off if the LN2 tank was already empty, and if NOTCam is moved to the service building where the ambient temperature is higher than in the dome. The cooling down is done in two steps: the PTR is run for 18-24 hours until the temperature is around -50 deg before filling with LN2. From the first LN2 fill it takes 40 hours to reach operating temperature: in practice cooling takes $\sim$ 3 days.

3.1.6 Temperature monitoring and warning systems

There is a continuous monitoring of the temperatures of the cold table, the central wheel section, the detector and the outer vessel as well as the pressure of the cryostat. The sensors are read every 5 minutes and values are logged and sent to a database retrievable for plotting. A cronjob checks every 15 minutes the last 3 entries and sends email warnings to staff if the detector temperature reaches a given limit and is increasing.

Since 2006 also the PTR cooling water is monitored. If the cooling water temperature exceeds 30 degrees Celsius or is below 10 degrees, the PTR will stop. A temperature sensor (# 367) is connected to the general TMS of the telescope. Email warnings are sent to staff if the cooling water exceeds its limits.

3.1.7 Maintenance and testing

Regular checks should be made of the holding time and the stabilization temperature when the LN2 tank is empty and cooling is maintained only by the PTR. It may vary from winter to summer, but should be around -175 to -190 degrees unless there are problems with the vacuum. The maintenance of the cryostat is described in Sect. 7.

3.2 Mechanics

3.2.1 Bearings

The wheels inside NOTCam with optical components (aperture, filter, grism, stop, and lens wheel) are driven by stepper motors and worm-gears whose bearings seem to have a lifetime of the order of two years. This lifetime is based on the use of NOTCam in the period 2001-2003. See Cox (2004) for a detailed description of the NOTCam bearings. All the bearings were exchanged in Nov-2003 and in Oct-2005, and while we keep using this same type of bearings (that need to be coated with the MoS_2 spray) this maintenance procedure should be continued every two years as a preventive means.

The User InterFace software was improved to allow the initialization of one wheel at a time in order to spare unnecessary turning of the wheels. Previously, all wheels had to be initialized when needing to initialize one.

3.3 Optical quality

3.3.1 The optical design

The optical design of NOTCam is documented by Atad (1997). Apart from the collimator, there are three lens systems, one pupil imager, one wide field (WF) camera and one high resolution (HR) camera. These three are mounted in the lens wheel and can be interchanged in a matter of seconds. The collimator focal length is 165 mm, that of the WF camera is 95.28 mm (F/6.35), and the HR focal length is 279.5 mm (F/18.63). The pixel scale for the WF camera is 0.23" and for the HR camera it is 0.08". The diffraction limit of the NOT is 0.12" in the J band (1.25 μm) and 0.2" in K (2.2 μm).

The collimator and the cameras are composed of multiple lenses made of BaF_2 or LiF. The BaF_2 lenses are coated and the LiF are not coated. The entrance window is made of IR grade fused silica.

3.3.2 The WF camera

The optical distortion of the WF camera is significant, especially in the corners. In 2004 a model of the distortion was made by M. Gålfalk based on his own good quality (FWHM=0.5") data on B335 and using 108 stars from the 2MASS point source catalogue. Fits files for download are available on the web page

`http://www.astro.su.se/~magnusg/NOTCam_dist/`

The model is presented in two images, of which one is the variable (delta_x 1024x1024) with information on how much each NOTCam pixel should be moved horisontally to remove the distortion (with sub-pixel accuracy) and another variable (delta_y 1024x1024) with the vertical displacement info for each pixel. (NB! Data stored since Jan-2006 have the x-axis flipped with respect to earlier. Therefore the sign must be inverted for such images.) This correction should be made to the raw data if you need high positional accuracy or if you are doing a raster scan and need to use the corners of each image. The distortion is up to 20 pixels in the worst corner.

For normal observations in dithered mode the edges are trimmed off, and in many cases extremely good astrometry is not required. Therefore the rigorous distortion correction described above is not always needed. Observations of a young cluster with the Science Array were used to test what positional accuracies one can expect by deriving the plate solution directly from a reduced NOTCam image by using the IRAF tasks *ccmap* and *cctran* and the 2MASS point source catalogue as a reference. The reduced NOTCam image is a combination of several dithered images, each skysubtracted and flatfielded, but no distortion corrected has been applied. In

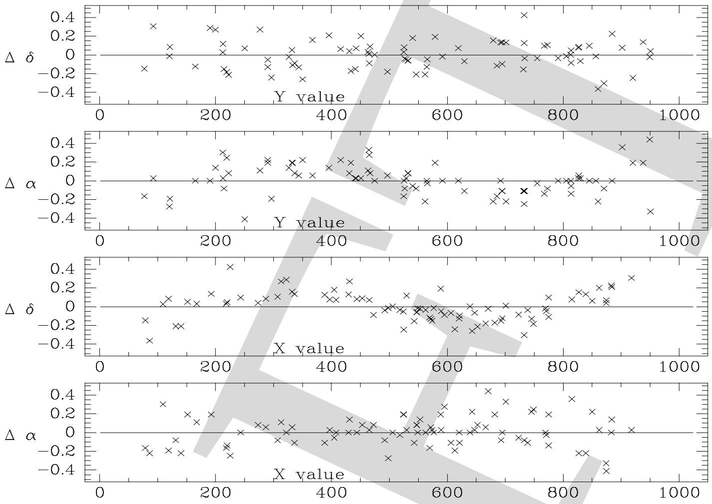

Figure 7: *The $\Delta\alpha$ and $\Delta\delta$ values plotted as functions of X and Y pixel position on the array. The standard deviation is 0.15" but the deviations increase towards the edges to $\sim$ 0.4". This is the astrometric accuracy obtained for the WF camera using* ccmap *in IRAF and 85 stars in the 2MASS database to make a plate solution. That is: no rigorous correction of the optical distortion has been made to the raw images.*

our test case the image is trimmed down from 1024 to 900 pixels because of the dithering applied. The 2MASS positions are reconstructed in the International Celestial Reference System (ICRS) via the Tycho 2 Catalog and are accurate to 0.08" over the range $9 < K_S < 14$ mag (Cutri et al. 2003).

First 85 stars were manually cross-correlated with the 2MASS catalogue (only 26 of these were brighter than $K_S = 14$ mag). The task *ccmap* was used with the **tnx** sky projection which allows for a distortion correction to be included. A general fitting geometry uses a surface polynomial of 3rd order in both x and y and full crossterms. Then a distortion surface is fit to the residuals from the linear part of the fit. The plate solution output gave a plate scale of 0.234"/pix in both X and Y. The rms of the RA/DEC coordinates were 0.15" and 0.14", respectively.

This plate solution was input to the task *cctran* which is used to transform all NOTCam XY positions to right ascension and declination ($\alpha\delta$). The NOTCam positions are then compared with the 2MASS positions. Table 4 shows the statistics, and Figure 7 plots the deviations as functions of X and Y position of the array. It is clear that the deviation increases towards the edges. Note that around 60 pixels are trimmed off each edge owing to the dithering observing strategy. The plate solution as output from *ccmap* is given in Appendix A.

Table 4: *The deviation between NOTCam positions and 2MASS positions of 83 stars over the NOTCam FOV. The deviation is given as* $\Delta\alpha = \alpha(NOTCam) - \alpha(2MASS)$ *and* $\Delta\delta = \delta(NOTCam) - \delta(2MASS)$ *in units of arcseconds.*

	mean	std dev	median	min	max
$\Delta\alpha$	0.012	0.16	0.00	-0.412	0.439
$\Delta\delta$	0.001	0.15	-0.014	-0.363	0.424

The plate scale and optical distortion should be re-determined after every operation inside NOTCam where the camera or the collimator have been taken out of their units, as well as whenever a new array has been installed.

It should be considered whether a rigorous distortion correction should be applied to all WF camera raw data as part of a future postprocessing.

3.3.3 The HR camera

Initially the HR camera did not produce a focused image at the detector focal plane, and the camera lens was shipped to the manufacturer Graseby Specac for adjustment. The modified camera was mounted in NOTCam Aug-2001, but still did not bring the image quite in focus in the slit plane. Before the commissioning of the spectroscopic mode the whole aperture unit had to be moved ~ 2 mm further away from the camera wheel.

The spatial resolution of the HR camera combined with good seeing frequently produced images with FWHM 0.3", but frequently also elongated stars not seen (i.e. not resolved) with the WF camera. This was initially believed to be due to a zenith dependence of the telescope astigmatism, as it always increased with larger zenith distance. Recently, the effect of elongated stars worsened dramatically and was seen in all imaging instruments at the NOT, and its cause has been found in corrections made to the pointing from a faulty look-up table in the TCS software. These corrections were disabled in August 2006. The HR camera plate scale and distortion should now be measured.

3.3.4 Ghosts and stray light

All filters in NOTCam are tilted by 6 degrees in order to minimize the amplitude of multiple reflections. WF camera images of (or very close to) very bright objects have not revealed any major problems with ghosts or stray light. A systematic search for ghosts by stepping around on a bright source was never made, though.

If HR camera imaging is made with the large open position in the aperture wheel then only about 7% of the light entering goes to the detector through the

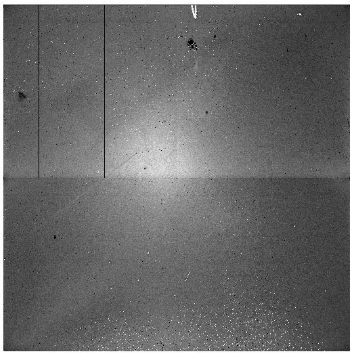

Figure 8: *HR-camera ratio image, domeflat without mask divided by image with mask. Intensity fraction is 1.7 in the centre and 1.3 in the corners.*

HR camera. Disturbing ghosts from bright stars located just outside the FOV have been observed. For imaging with the HR camera it is therefore recommended to use a small square mask in the aperture wheel (named *HR imaging*). It was made and installed in 2003 to fit the HR FOV and diminish any stray light and ghosts. The stray light contribution in dome flats went down by 50% when using this mask. Also, the background became more uniform (i.e. the centrally peaked background emission disappeared), see ratio image shown in Fig. 8.

3.4 Focus

3.4.1 Internal camera focus

The internal focus of NOTCam is set by moving the detector plate with respect to the camera wheel. Upon initialization the detector plate moves to its furthest distance from the camera wheel (camera focus unit ~ 0). The freedom of movement for the detector plate is 5.5 mm or 6100 camera focus units. The flexure was measured at IJAF to be 25 μm. Some focus travel with wavelength is expected. According to the optical design (Atad 1997) the detector distance should move by 0.78 mm by going from 1.04 to 2.2 μm (Y to K band) for the WF camera, and by as much as 5.66 mm for the HR camera. During commissioning of the imaging mode in 2001 the internal focus was measured with the small (50 μm) pinhole. The HR camera was entirely outside the focal range of the mechanism and a mechanical adjustment of the instrument was needed before commissioning of the spectroscopic mode (the whole aperture unit had to be displaced by 2 mm away from the collimator). The WF camera was outside the focal range for the bluest filter (Y). It was therefore decided to fix the camera foci for imaging mode and adjust the telescope focus.

For imaging mode the internal focus is set to the default values of **1** and **5650**, for the HR and WF camera, respectively. The telescope focus is then adjusted from night to night, and also for filter changes. With the future implementation of the "Sequencer", filter and focus changes can be scripted.

For spectroscopic mode it is necessary to have the slits in focus, and there is a different focus for each slit/filter combination. See the Commissioning Report for Spectroscopic mode (Telting 2004) for details. In this mode, focusing is done by selecting the right internal focus according to slit and filter used, and then to find the appropriate telescope focus value. The telescope focus is then kept fixed and the internal focus is modified according to the pre-measured values for each slit and filter combination.

The internal focus should be re-measured using the Hartmann masks every time a new array has been installed, or other operations made inside NOTCam that might affect the focus.

3.4.2 The focus pyramid

Based on the success with the focus pyramid for ALFOSC, a focus pyramid for NOTCam was designed by Michael Andersen and made by Microglass APS in Denmark. A holder for mounting the pyramid in the grism wheel was made by the instrument group at CUO. The optical material is "Infrasil 302" from Heraeus glued together with vacuum grade cement to form a pyramid of 25 mm diameter. A metal frame with springs keeps the pyramid together if the cement should give up. According to tests in the lab at the CUO to check the endurance of the cement, the material showed no sign of stress after numerous thermal cycles. Outgassing, however, was not easy to check. The pyramid was installed in the grism wheel in NOTCam in Nov-2004. A post-processing script similar to that for the ALFOSC pyramid was made and the unit was calibrated. The calibration consists in finding the best focus and the corresponding distance between the 4 stellar components split by the pyramid (the reference distance). The scale factor is the relation between the telescope focus units and the distance.

Table 5: *Calibration parameters for the focus pyramid. Also the date of the measurement, the filter used, and the average seeing is given.*

Camera	Scale factor	Ref. Distance (pixels)	Date	FWHM (")	Fil
WF	36.04	27.65	15.06.2005	0.6	Ks
HR	11.6 ±0.19	79.3 ±0.5	28.08.2006	0.33	Ks

Through focus tests were made in Jun-05 and Aug-05 to finetune the calibration

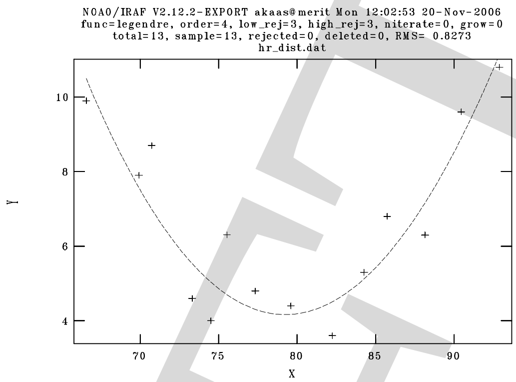

Figure 9: *Calibration of the focus pyramid reference distance for the HR camera. The distance in pixels on the x-axis and the FWHM in pixels on the Y-axis (4 pixels FWHM corresponds to 0.32").*

of both cameras. (There was no opportunity to do this during the half year that the science array was mounted.) Another test with the engineering grade array in Aug-06 confirmed previous calibration and only minor adjustments were made to the HR camera parameters. See Fig. 9 and Table 5.

We recommend focusing with the focus pyramid in the Ks band and then use the pre-determined offsets for the other filters. The values in Table 6 were found in very good seeing conditions.

Because of the unknown long-term behaviour of the cement it is recommended to make through-focus tests for both cameras about once per year, in good and stable seeing conditions. If the array is exchanged, the pyramid should be recalibrated,

Table 6: *Focus offset values between filters to be used with the TCS command* **foc-del**. *Obtained in good seeing (0.3-0.5").*

TCS command	WF-cam	HR-cam	
	5650	1	Internal camera focus (fixed)
foc-pos	23480	23570	Telescope focus value for **K,K',Ks**
foc-del	0	0	**K,K',Ks**
foc-del	-30	-35	**H**
foc-del	-75	-90	**J**
foc-del	-145	-170	**Yn**

although it should work well if the internal focus stays the same. See Sect. 7.2 for how to perform the through-focus observations needed for the calibration.

3.5 Filters

There is space for 30 filters at any time in the two filter wheels with 16 positions each. The slots are made slanted such that all filters will be mounted with a tilt of 6 degrees in order to minimize multiple reflections. The filters have an allowed range of 25±0.5 mm diameter and can be at most 5 mm thick. The spare set of JHK filters are currently mounted in the stop wheel for test/calibration purposes, but are not tilted.

3.5.1 Transmission curves

All NOTCam filters are scanned with grism#1 in NOTCam (i.e. in vacuum and cold at T = 74 K). Updated transmission curves are available on the web. These calibrations were made through the 1 mm pinhole (7.33") to improve the background subtraction and thereby the accuracy of the transmission. This means, however, that the transmission curves are correspondingly smoothed. The wavelength calibration was made with the 128 μm slit, however, and the offset between the slit and the pinhole position was corrected for.

3.5.2 Narrow band filter vignetting

Narrow band filters are still to be tested for the sensitivity across the FOV, or vignetting, because of the expected slight change in wavelength across the field.

3.6 Flat fields

The flat field looks about the same for all filters in NOTCam. Its morphology is dominated by the pixel to pixel sensitivity variations of the array. For the engineering grade array these sensitivity variations are large with a broad diagonal band of 20% brighter than the average and a dark corner 15% fainter. The small scale pixel-to-pixel variations measured in 20×20 pixel boxes is 3-4%. The science array is much flatter: only ±5% across the whole field and 2% in the small scale. The sensitivity of the array is only slightly wavelength dependent, all filters have the same size, they do not vignet the FOV, and they are permanently mounted in the parallel beam inside a clean vacuum cryostat. There are filter to filter differences, however, of the order of 1 % for the science array on 14/1-2006.

Considering that 90% of the NOTCam time is used with the WF camera, and that a substantial fraction of this time is spent using the standard broad-band filters, it is suggested to do a regular check on the $YnJHKs$ flat fields obtained

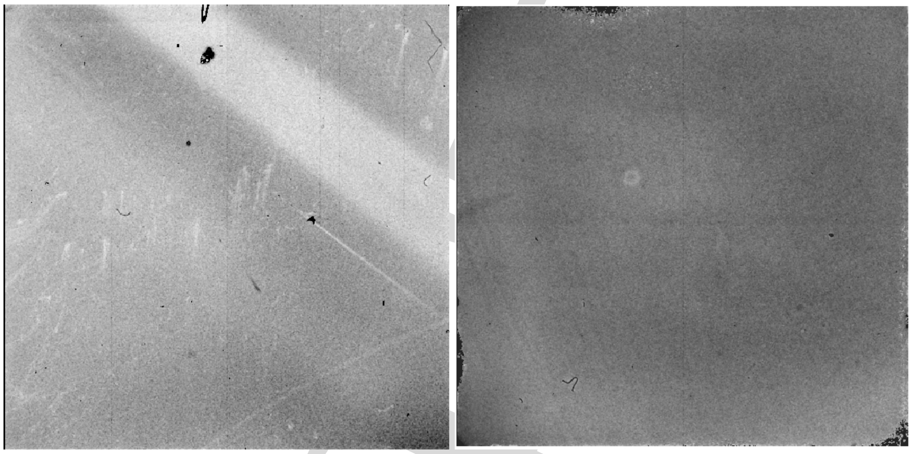

Figure 10: *The flat field appearance for the Engineering Grade Array (left) and the Science Array (right). Both are master flats in the K band obtained from differential skyflats.*

with the WF camera. For NOTCam the recommended flat fielding strategy is to use **differential flats**. Note! Until the behaviour of the dark is properly understood and the problems inherent to the electronics configuration are fixed, we recommend users to avoid separate dark subtraction. The dark is subtracted out automatically in the sky subtraction. We emphasize that darks taken daytime are perhaps not a good representation of the dark at the moment of observations. Therefore, flats should not be constructed from the dithered observations themselves, a method which is otherwise frequently used. For NOTCam imaging we recommend differential flats because both the dark, the thermal background, and possible straylight components are efficiently removed from the flat field this way. Differential **twilight** flats are preferred to differential dome flats (lamp ON - OFF) because of the structures inside the NOT dome.

The monitoring of the WF camera flat field for the $YnJHKs$ should consist of taking differential sky flats once per NOTCam technical night whenever the weather permits. The requirements are simply to go to a blank field, set the correct filter, and run an observing script twice for each filter, cycling in the order $KsYnHJ - KsYnHJ$ (for evening twilight, oppositely for morning twilight) to get bright and faint pairs. The analysing script should sort and order the images, subtract differential pairs, median combine with additive scaling, smooth by 3x3 pixel to get rid of individual bad pixels, and finally produce normalized master flat per filter. Simple statistics should be output to a database table to give the percentage of deviation from flatness (in small areas as well as over the whole array).

This opens up for an additional possibility of making a **flat field archive** by simply storing the master flat fields as fits files in an on-line archive. In a very simple fashion this has already been done since 2003 (i.e. gzipped fits files are available from the web page www.not.iac.es/instruments/notcam/flats/). In a proper archive linked to a database these can be of use for quick-look reductions at the telescope. Also, they may be used in the case of lost opportunity to take twilight flats during an observing run. Possibly archive sky flats are better than dome flats on the same day, but this depends on the flat field stability.

To monitor short-term effects in the flat fields the new flat should be divided by the previous flat in the database and this ratio image should also be archived. Alternatively, one could leave the flat field quality monitoring to the domeflats obtained with the J-band during the detector quality control. These tests are performed more frequently, and the data is taken daytime. The drawback is the limitation to one filter. In addition, the archive of $YnJHKs$ twilight flats is probably quite useful for more purposes than mere monitoring.

Usually the stability of the flats is of the order of 1-2 % over several months, but if the cryostat has been opened there is more likely to be changes in the distribution of particles.

3.7 The shutter

3.7.1 Initial problems

NOTCam is one of the few infrared cameras which has a shutter. Normally the integration time in IR cameras is defined by the difference between the "post" and the "pre" exposure reads. A fast shutter operating at -200° C is challenging. The NOTCam shutter lost synchronization frequently during the first half year at the NOT. The problem was first thought to be related to the spring holding the microswitch down being so strong that it would push the shutter back a short distance after initialising. This spring was weakened. Also, a LED box diagnostics device (the so-called "buzzer") was connected to monitor the shutter behaviour. The shutter continued to misbehave, and the microswitch spring was further weakened. After this the shutter worked perfectly in warm conditions. But it continued to fail at operating temperature. Finally the problem was solved by realizing that the shutter speed requested by the software was too high for the motor.

The shutter is a rotating disk (of two aluminized plastic sheets) of the "butterfly" type (two open and two closed positions). It always rotates in the same direction. The action from closed to open or vice versa is always one 90 degree turn of the disk. The maximum shutter speed was calculated by Cox (1998) to be 187 ms per 90 degree rotation based on the motor torques. At the handover of the instrument, however, the speed requested by the software had been set to 100 ms. By increasing the time from 100 to 150 ms (in Nov 2001) all shutter failures disappeared.

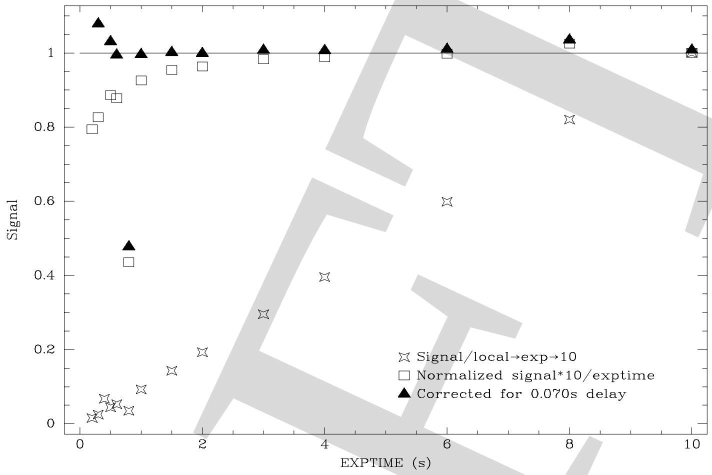

Figure 11: *Shutter timing test shows: the signal per exptime corrected for dark level and lamp variations (open stars), this signal normalized by exposure time (open squares), and normalized signal corrected for a 0.070s shutter delay (filled triangles).*

3.7.2 Shutter accuracy

The shutter accuracy was initially found to be acceptable for exposure times as short as ~ 2 seconds (i.e. within $\sim 3\%$) and better than 1% for exposure times > 3 seconds. For most purposes and in order to be sky noise limited and minimize the overhead to readout (readout time = 2 x 3.6s), the exposure times with NOTCam are usually > 2 seconds, even for broad band imaging. With the ramp-sampling mode the minium exptime is 3.6 seconds.

For science projects on very bright targets where defocusing is not a viable solution, however, shorter exposure times are needed (in spite of the large overheads). Here it is vital to know the shutter accuracy. In 2006 the shutter was calibrated with data obtained with the script **shutter.run**, and the results are shown in Fig 11. Disregarding three points which gave spurious values[2], a shutter delay of 0.070 seconds was calculated. Implementing this correction on the data points, the shutter should be accurate to within 1% for exposure times as short as 0.6 seconds. Exposure times shorter than 0.6 seconds are not reliable, and since the ramp-up time for each shutter movement (open and close) is 150 ms, the absolute minimum exposure time that can be handled must be somewhat larger than 0.3 seconds. There is no software

[2]The reason for the three deviating points may be related to jumps in the dark levels (which was the case for the 0.8s exposure) or rapid variations of the lamp which could not be corrected for.

Table 7: *The NOTCam broad band filters considered for zero point monitoring.*

Name	λ_{on} (μm)	λ_c (μm)	λ_{off} (μm)	$\Delta\lambda$ (μm)	Comments
Y_n	0.996	1.033	1.069	0.073	$\sim$ 50% narrower than UKIRT Y
J_{MKO}	1.165	1.246	1.328	0.163	26% narrower than 2MASS J
H_{MKO}	1.484	1.632	1.780	0.296	7.5% broader than 2MASS H
K_S	1.990	2.145	2.300	0.310	9% broader than 2MASS K_S
K_{MKO}	2.030	2.198	2.366	0.336	

limit on the **exp** command in BIAS. The user should know that by giving an **exp t** command with $\mathbf{t} < 0.6$ the true exptime used is not known.

The accuracy of the shutter should be checked about once per year. A stable calibration lamp would be desirable. Currently, one has to monitor the lamp along the test, for instance by taking repetitive 10 second exposures in between each of the shutter test exposures. Because of the strangely behaving darks one should take darks of the same integration time right before each exposure. In between each different light level clean the array well to erase any contribution from the memory effect. See Sect. 7.4 for a description of the testing.

3.8 Efficiency and throughput

Monitoring of the photometric zeropoints should be done by regular measurements of a set of NIR photometric standard fields in given broad band filters. This keeps track of the combined effect of the telescope + instrument throughput and the detector quantum efficiency. It should be sufficient to do this with the WF camera only, as the only difference between the HR and WF mode is the camera lens, which is not very likely to change its performance. The most likely quantity to vary is the telescope mirror reflectivity. There is also a possibility of a long-term degradation of the QE of the IR array detector. Separating these two effects can be done using our monitoring of the zeropoints in the optical (with ALFOSC and StanCam) and the expected reflectivity of aluminium as a function of wavelength.

3.8.1 Choice of pass bands

Below we discuss the choice of filters to be included in the monitoring in order to 1) sample well the response curve of the QE of the detector, and 2) possibly serve as a useful reference to the community (in a future version).

Until a decision has been made about ordering the two new broad band filters $Z(0.84 - 0.93\mu)$ and $Y(0.97 - 1.07\mu)$ we suggest including the Y_n filter to trace the

Table 8: *The Teide Observatory atmospheric extinction coefficients in the NIR as given by Fuensalida & Alonso (1998).*

Band	mean	std dev	median	mode
J	0.161	0.009	0.127	0.086
H	0.099	0.008	0.065	0.065
K	0.120	0.006	0.093	0.080

zero-point also at the blue end of the IR array response function. Considering the usefulness of the new Y filter in terms of brown dwarf studies and very high redshift objects, it might become a frequently used passband, and the UK Infrared Deep Sky Survey (UKIDSS) with the WFCAM is performed in the 5 band passes $ZYJHK$.

The K_S filter is suggested instead of the standard K filter because it has a shorter cut-off wavelength and thereby less of the thermal component of the background passes through. For this reason it is probably more frequently used by the community. (A K_S filter is also used by 2MASS, but note that it is slightly narrower than the NOTCam K_S.) The K' filter is not considered, because although the thermal component is equally low as for the K_S filter, its passband extends into highly variable water-vapour transmission regions at the blue end. It is mainly designed for very dry and high sites, such as Mauna Kea (Glass, 1999).

3.8.2 Accuracies and observational requirements

Although atmospheric extinction is relatively small in the near-IR, the local "calima" of dust from Sahara can produce strong variations, and it would be interesting to separate this effect from variations in the instrument + telescope throughput. There are no published measurements of the atmospheric extinction in the near-IR at the Roque de Los Muchachos. Fuensalida & Alonso (1998) describe the JHK extinction data obtained in the period 1989 to 1997 at the 1.5m Telescopio Carlos Sánchez (TCS) at the Teide Observatory. These values are very similar to other observatory sites such as Mauna Kea. We use their statistical mode values (see Table 8) when we have too few measurements to determine the nightly extinction coefficients from our data.

We suggest that the same standard field should be measured at least twice, preferably three times, at different air masses per night. The "small" airmass should never be larger than 1.3 (i.e. zenith angles < 40 degrees), but preferably as small as possible. The selected standards cover a range in right ascension such that at any moment there are fields available at airmasses smaller than 1.3.

The observations should always be made by dithering the stars on five different positions on the array. This will allow for a proper sky estimate and subsequent subtraction, as well as a median filtering of bad pixels. Also, the inaccuracies in the flat field - which is the dominating source of errors in NIR photometry - will be taken into account in the measurement of the scatter. Autoguiding should be ON to make the teloffsets accurate such that the image shifts can be automatized in the reduction scripts.

3.8.3 Calculations of the zero points

Since the purpose of this calibration in principle is to track the behaviour of the throughput, which is a detector-, instrument-, and telescope dependent quantity (where most likely the telescope mirrors reflectivity will dominate). Thus the zero-points are not meant to serve as a photometric calibration for the user community. We suggest to calculate the **zenith** zero point magnitudes in the **natural "NOT-Cam system"**, i.e. no colour coefficients are included and no attempt is made to extrapolate to outside the atmosphere.

The transformation equations are thus on the simple format:

$$M_{cal} = M_{inst} + ZP - A * (X - 1.0) \tag{2}$$

for each pass band, where M_{cal} is the calibrated magnitude, M_{inst} is the instrumental magnitude, ZP is the zero point magnitude, A the extinction coefficient (mag/airmass), and X is the airmass.

3.8.4 Photometric scatter over the FOV

The photometric scatter for the Science Array was preliminarily measured with 5-point dithers of the standard star UKIRT FS 122 (GSPC P161-D) in the JHK_S bands. The distance between the 5 dithers were 15". A full test on 16 positions over the whole array is pending.

Table 9: *The photometric scatter across the FOV. Measured on 5-point dithers with aperture photometry (aperture radius = 20 pix or 4.7").*

Band	mean	std dev	median	N
J	11.668	0.013	11.668	5
H	11.392	0.012	11.393	5
K_S	11.352	0.015	11.347	5

3.9 NOTCam overheads

The various NOTCam overheads are currently summarized in Table 10. Some of these quantities (such as image storage and telescope dither times) may vary and should be monitored.

Table 10: *Overheads for NOTCam observations.*

Readout time	2 x 3.6 sec
Image storage (4-32 MB files)	2 - 6 sec
Clean-array command **clear**	3.5 sec
Changing between WF and HR camera	$\sim$ 60 sec
Changing filter	2-30 sec
Changing grism	2-30 sec
Changing slit/mask	tbd
Telescope dither 10-15” with **ag-on**	6-7 sec
Telescope dither 10-15” with **ag-off**	tbd
Telescope dither 100” with **ag-on**	tbd
Telescope dither 100” with **ag-off**	10 sec
Focusing in imaging mode	<5 min
Taking twilight flats in JHK	$\sim$ 20 min

4 The NOTCam detector Quality Control

4.1 The already implemented detector QC

The NOTCam *detector* Quality Control project is based on a series of domeflats and darks taken during daytime by running a script under NOTCam BIAS and thereafter an analysing script which calculates and sends the results to a database and updates a www page.

Several detector characteristics such as the read noise level, the gain, the reset level, the linear range, the amount of bad pixels, and the dark current can be found with this QC.

The only requirements are:

- NOTCam must be mounted on the telescope
- a person must open mirror cover, turn on lamp, and start the script
- nobody can enter the dome while data is obtained (1.5 hours)
- a person must execute the analysing script and check that the results are ok

It is important that the results are checked. Possible problems such as pick-up noise or drifts in the reset levels will be detected immediately by looking at the results.

An analysing script was written in IDL by Silva Järvinen in 2002-2003. Since Jan-2003 we have run the NOTCam detector QC and created a substantial data base for the Engineering Grade Array. In the period Oct-2005 to Apr-2006 the Science Grade Array was in use and a new data base was started for this array. All the data is available on-line in graphic and tabular format. At the time of writing the detector QC calculates the following for each readout mode:

- The gain and readout noise (with errors) per quadrant. Uses Janesick's method on short darks and bright domeflats. For the reset-read-read mode zero exposure darks are used, while for the ramp-sampling mode the shortest available are 4.2 second darks.
- For each quadrant the range of linear behaviour is calculated, i.e. the maximum number of ADUs which gives linear response. Two limits are calculated, linearity to within 1% and 3%.
- The amount of bad pixels is given in percentage. Zero pixels, hot pixels, and cold pixels are monitored separately.
- A JPG image map of the zero pixels is produced.

- The detector temperature taken from fits header keyword
- The dark current as a function of exp time

More details regarding how the analysing script currently works are found in the web document

`http://www.not.iac.es/instruments/qc/notcam_document.html`

Currently, we use a single 40W bulb on the floor beneath the instrument (since using the dome bulbs adjusted down to sufficiently low light levels makes them flicker). The 40 W bulb gives around 600 ADUs in 0.5s in the J band. The right setup to use is found in the instructions on the web. The data are obtained by running the script **lintest.run** which takes 1.5 hour and includes both readout modes.

Then the automatic IDL reduction script must be started. It calculates and sends the results to a database and updates the www page in a total of about 5 minutes.

4.2 Suggested upgrade

Suggested improvements to be made:

- change s/w from IDL to python/pyraf ?
- improve database to allow flagging of deviating points (no data should be erased, but not all data should be used in the calculations of average values)
- include monitoring of the reset level. No additional data is required. The median value of the central 200 x 200 pixels in each quadrant should be stored in the database. Make a new 4 window plot to show values.
- add date when data was obtained (currently the stored date refers to when the analysis was made)
- output a badpixel file (for example a mask image in FITS format) with all the bad pixels (hot, cold and dead with different number coding) found with a given exp time. It should go to an archive with downloadable bad pixel masks (FITS). No additional data needed.
- improve the calculation of the read noise for the ramp-sampling mode in order to take into account the linear regression analysis. No additional data needed. Up to now it is measured on the first readout and the readnoise therefore appears to be the same as for the reset-read-read mode. The readnoise should be measured as a function of multiple reads. Probably by looking pixel by pixel at the deviation from the linear regression result.

- output master darks for a set of exptimes to be stored in an on-line archive (assuming an electronics upgrade gets rid of the high and variable dark measurements)
- upgrade to a suitable and stable lamp
- calculate the deviations from linearity to allow for linearity correction of the data (this should preferably be done pixel by pixel)
- consider monitoring the J-band dome flat by storing the master flat and making a ratio image with the previous flat in the archive (no additional data needed)

None of the suggested improvements need any modification to the observing script for the detector QC (**lintest.run**).

5 The NOTCam imaging Quality Control

We recommend that the NOTCam *imaging* Quality Control (QC) project monitors the following:

1. $YnJHKs$ zeropoint magnitudes
2. $YnJHKs$ sky backgrounds
3. $YnJHKs$ atmospheric extinction
4. $YnJHKs$ flat field quality

These quantities are found from two types of observations:

- twilight flats
- photometric standard stars

It is suggested to do the zero point monitoring for NOTCam through the broad band filters $YnJHKs$ (see Sect. 3).

5.1 Twilight flats

On every NOTCam technical night whenever the weather permits, differential twilight sky flats should be obtained in the filters $YnJHKs$ with the WF camera. These flats are needed in any case for the $YnJHKs$ zero point monitoring described below. However, they also serve as input to the suggested long-term flat field accuracy monitoring, and the flat field archive.

The data are obtained by going to a blank field, cycling the filters in the order $KsYnHJ - KsYnHJ$ (for evening twilight, and oppositely for morning twilight) and running the script **skyflat.run** for each filter/cycle. This script makes 10" telescope offsets to enable filtering away stars. The exptime must be kept constant for each filter, otherwise the differential pairs can not be used to subtract correctly the thermal, stray light and dark contributions.

5.2 Photometric standard stars ($YnJHKs$)

In Sect. 3 we suggest to do the zero point monitoring for NOTCam for the WF camera through the broad band filters $YnJHKs$. A set of six standard star fields from Hunt et al. (1998, AJ 115, 2594) have been chosen as follows:

- to have standards available at the NOT at any time with zenith distances less than 40 degrees (airmass < 1.3)

- to have 2 or more standards per field
- standard star was measured over a minimum of 4 different nights
- standards have published photometric errors < 0.024 mag
- to have magnitudes in the range 9.4-13.5

For the Yn band there are no good standard measurements yet, but we will tie it up to results from the UKIRT survey (Dye et al. 2006). This band is much narrower than the others, but the exposure time chosen should be sufficient to give a reasonable signal to noise ratio.

One observing script is made per standard field, and this same script is run for all filters. For instance for the standard AS05 use **as05_qc.run**. Auto-guiding should be ON. (The reason for this is that the reductions depend on the initial shifts calculated from the teloffset size in the observing scripts. These may be totally wrong if not autoguiding.) For the reduction purposes it is vital to use these scripts as they are, except for the exposure mode which can be changed without problems if needed. The teloffsets used make sure the telescope points back to the same starting position. This is important for the reduction script **std_qc.cl** described below. The exposure times have been chosen to avoid entering the non-linear regime (i.e. where the deviation from linearity is more than 1%), even for cases of very good seeing. All standards are observed in a 5-point dithering. The total time for all four filters is from 12-16 minutes per standard.

The zeropoint monitoring observations should be performed every NOTCam technical night which has clear/photometric weather. At least one standard field should be observed and this same should be repeated at three different airmasses, if possible. Also, differential twilight sky flats should be obtained for $YnJHKs$ using the script **skyflat.run** (see above).

5.3 Data reduction

The data will be processed through a set of IRAF scripts. A data flow chart is shown in Fig 12.

5.3.1 Flat field images

The skyflat data reduction is done with the script **mkflat_qc.cl** which needs an input date prefix (e.g. NCph28), and the user is queried about camera and filter selection. The calling sequence is: **mkflat_qc prefix filter camera**, for instance:

```
mkflat_qc NCph28 ks wf
```

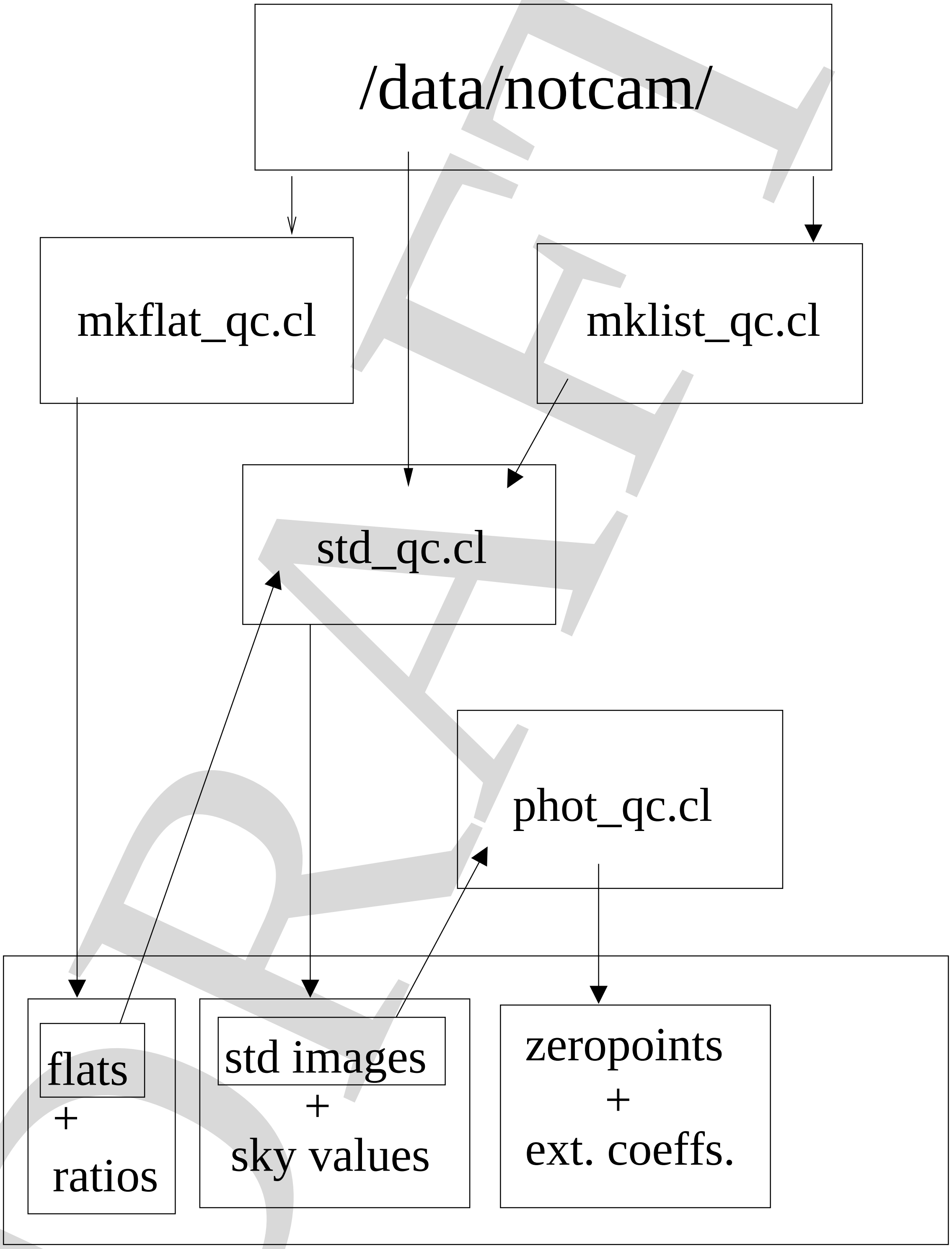

Figure 12: *Imaging QC data flow chart.*

for making a WF camera Ks masterflat for the date "ph28" (the standard NOT data file naming convention). The script can be used for all differential raw flats, i.e. both dome lamp (ON-OFF) flats as well as twilight (bright- faint) flats. The script selects the flat images according to selected filter and camera, orders then the flats in decreasing brightness, makes difference pairs, median combines these with an additive scaling to a master flat, smoothes the image with a 3×3 pixel median filter to minimize individual bad pixels, and normalises the master flat. The script takes ~ 10 seconds to run, but it has to be run for each filter.

The output master flat is displayed on a DS9 and the fits file is stored locally. The script outputs some image statistics to quantify the small scale pixel to pixel flat quality, i.e. standard deviation in 11 small (20x20 pixel) boxes. A plot is made of two image diagonals to show the deviation from flatness over the whole FOV. The flat field quality can be determined by the user based upon these numbers and reference values which are also given. The master flat is stored in the on-line flatfield archive if/when the user decides that the result is satisfactory. Reasons for non-satisfactory flats may be: cloudy sky, or non-removal of stars because dithering was not made (happens if the rpc access code is forgotten), or forgetting to turn off the dome lamps, etc.

The master flat is stored with a name of the form: **ph28_sf_wf_yn_eng** which tells the date, whether it is a twilight or dome flat (sf or df), the camera used (WF or HR), the filter (Yn, J, H or Ks), and which array (eng, sci, or sci2). Other necessary information is stored the fits image or header. The new master flat is divided by the second newest in the archive (for the same filter, camera and array) and a ratio image is obtained with the name **ph28_sf_wf_yn_eng_r**. This image will show any changes of the flat field since the last Imaging QC. A plot could be updated with the last acquired value for the small-scale standard deviation per filter, for a quick overview of long term effects. However, the best way to judge the flat fields is to check the ratio images.

Note that the $YnJHKs$ master flats produced above are used as input files in the standard star reduction. The input name of the flat to use can be typed in manually or alternatively it can be made such that the task looks for the latest archive flat for a given filter as the default input flat.

5.3.2 Standard star images

For the reductions of the standards a script **mklist_qc.cl** is first run to select and sort the standard star observations in image lists. Note that the standard star observations must have FITS keyword IMTYPE = STD as set in the observing scripts. The image lists are called for instance "as05_ks_1", meaning the first observation in the Ks filter of AS05, and are used as input to the standard star reduction script.

The script **std_qc.cl** reduces one 5-point dither at the time. It evaluates the sky frame, does the (scaled) sky subtraction, the flat fielding, and finally the image shifts and median combination, to produce one combined image per 5 point dither. Both in the construction of the sky image and in the final combination of the shifted and reduced images the IRAF task *imcombine* is used. It takes as input an image list and a flat field. Rough input values for the shifts are taken from the teloffset values used in the observing script (fixed values). In order to find and center the stars to be used for the accurate calculation of the shifts, a call to the IRAF task *daofind* is used on the sky-subtracted and flat corrected first image in the list. The calling sequence is **std_qc imlist flat**, for instance:

```
std_qc as05_ks_1 ph28_sf_wf_ks_eng
```

The output name of the resulting image is constructed from the prefix date, the standard name, and the filter and is suggested to be on the form **ph28_as05_1_yn**. The individual images have the same name, but concatenated with **001-005**. (The individual images are stored for the possible calculation of the internal scatter in the photometric measurements as a function of array position. This is not yet implemented.) All temporary images are deleted at the end of the script. The result image is displayed on a DS9 when the script finishes.

The script **std_qc.cl** can be run manually, once per standard star observation and filter (meaning it has to be done up to 12 times), or it can be run as a batch job for all standards with repeated calls to **std_qc.cl**. This last mode is not yet functional, but should be easy to implement to streamline the analysis.

5.3.3 Aperture photometry

When all the standard star images are reduced the photometric analysis is made with the script **phot_qc.cl** which does aperture photometry (with large apertures) and outputs the zeropoints and the extinction coefficients (if calculated) to the archive database. This part of the analysis is for the time being interactive, in the sense that the correct standard star(s) must be located by the user by putting the cursor on it/them in the right order. The input is the list of standard star reduced images:

```
phot_qc ph28_as*.fits
```

The script **phot_qc.cl** does the following:

- For each image makes a call to the IRAF task “digiphot.apphot.phot” to do aperture photometry through a number of different apertures
- Sorts the output magnitude files
- Calculates the measured photometric scatter over the FOV

- Makes the obsfile and sets up the apcor files etc.
- Finds image shifts between repeated observations using the IRAF task *daofind*.
- Calculates the zeropoints using fitparams

(Some finetuning of this script is still needed...) In the end the zeropoints and the extinction coefficients are calculated. If there are too few data points to calculate the extinction coefficients, then we use the standard values 0.086, 0.065, and 0.08 for JHK.

A standard star catalogue and a configuration file for the used transformations (stored on the local disk on *elena*) are used for the photometric calibration.

5.3.4 Data storage

All input images are taken from **/data/notcam**, i.e. the image lists created with **mklist_qc.cl** use this as the input file path.

Storing only the master flats and their ratio images results in 8 MB per Imaging QC. Imaging QC is foreseen to be done around six times per year, but depends on the scheduling of NOTCam technical nights and on the availability of photometric weather.

It still needs to be defined how the output information from the scripts is to be piped to the on-line archive, as well as the exact design of the database. Apart from the output fits images this includes also values such as average sky background values per filter (which later can be plotted versus distance from the moon), zero-point magnitudes and errors, measured extinction coefficients, small-scale standard deviation in flats.

6 Tests upon mounting on the telescope

After having mounted NOTCam on the telescope the following tests must be done before the instrument is handed over for observations. Normally the first night of mounting is a technical night, and if not, then the observer will have to spare some of the first minutes of the night (after the flats have been taken).

The so-called "first night" tests listed below have been performed regularly since 2003. The first three tests are daytime tests and the last three are tests to be made on the sky:

1. Check the optical alignment of wheels if the instrument has been opened and any units dissembled inside NOTCam. Use the pupil imager to check that filters and stops are aligned with the pupil. If not, adjust wheel positions by changing the motor units in the appropriate **.def** files in *marissa* in the directory **/home/softremote/notcam/tcl-uif/**.

2. For each camera check the position of the small 50μm pinhole on the array if NOTCam has been opened since the last measurement. Open the mirror cover (**o-m-c** on the TCS) and turn on some light in the dome. Use the K_S filter. Set the internal focus correctly according to camera. Find the pinhole position and update the webpage log. Remember to use the stored images (i.e. the postprocessing DS9) rather than the BIAS buffer image (BIAS DS9) to have the pixel values right, otherwise the flip in X-axis will make confusion.

3. Run the **Detector QC**. The content and procedure is described in detail in Sect. 4. Setup the instrument correctly, open the mirror covers, turn the NOTCam QC calibration lamp on and run the script **lintest.run**. It takes 1.5 hours and produces 168 files.

4. Determine the rotation centre on the array for both cameras. This must be done on sky. After having done flat fields go to a focus star. When you have focused the telescope and stored an image of the star with default **field-r -90**, then rotate to **field-r 0**, take another image, rotate back to **field-r -90** and take yet another image to have an estimate of the presicion. Save all images. This should be done for both cameras. Later you can identify one or more stars in each image and find from this the X,Y values for the centre of rotation.

5. Determine the instrument alignment on the sky. This is done for the WF camera only. Use a focus star close to zenith, set default **field-r -90**, and place the star on detector position [X,Y] = [200,600] as seen in stored images (i.e. the postprocessing DS9). Take an image, and save all images. Make a **teloffset 140 0** command. This should move your star to around [X,Y] $\sim$ [800,600]. Take another exposure. Move back with **teloffset -140 0** and

expose again. Measure with **imexam** the position of the star in all images. The telescope movement will not have been exactly along a row. Determine the small angle between the two positions from **arctan(dY/dX)**. This is the offset angle from the **field-r -90** value. For the engineering grade array it has been from -0.3 to -0.9 degrees giving an exact field angle of -90.3 to -90.9 in order to have the detector rows/columns properly aligned with the sky orientations. Update the webpage log with the correct field angle. Currently we do not adjust the field angle to have the detector aligned on the sky, but the offset angle must be known to align the slits properly.

6. Because of the need for dithering along slit with IR spectroscopy, we have selected to keep the fiducial field rotation **field-r -90** and tilt the slits slightly to correspond to the above found offset angle. Then it is easy to do the dithering along slit while observing with a simple **teloffset x 0** command in the observing script. If the offset angle has changed from previous time, then the slits need to be realigned. If spectroscopic mode is not going to be used on this night, this can in principle be done daytime using the images found above for the alignment. Change the slit alignment by updating the stepper motor values in the file **/home/softremote/notcam/tcl-uif/slit.def** on *marissa*. For details see the procedure on the NOTCam spectroscopy webpage.

7 Annual tests

7.1 Vacuum cryostat health checks

The vacuum of the cryostat is continuously monitored together with the temperature of the detector, the central wheel section, the cold table, and the outer vessel in the NOTCam logging which has been running since 2001. The sampling time is 5 min. Recently, a continous logging of the temperature of the cooling water used by the PTR was also started. These systems send warnings by email to staff when values are out of range.

The health of the vacuum cryostat depends critically on the way it is handled while open. It should always be opened in the clean room, and care should be taken to operate NOTCam with clean hands and to clean every item which is installed. These instructions are available on the web. Always bake the getter when NOTCam is openend, and make sure it is installed hot, and that the vacuum pumping is started as soon as possible after.

As a regular maintenance of the PTR two units (an oil adsorber for the compressor CW303 and a M201 rotatary valve) should be exchanged every 15000 hours running.

At opportunity (between visitor runs) when NOTCam is kept cold it can be tested for holding time, stabilization temperature and vacuum while depending on PTR cooling only. The test is simply to make sure NOTCam is not filled with LN2 (set the temperature limit in the cronjob to -175 to avoid email warnings) and follow the behaviour by plotting the logs. This takes about one week.

7.2 Focus pyramid

A full through focus test for both cameras should be made in good and stable seeing conditions.

- Use a suitable star on the meridian and at small zenith distance ($<$ 30 degrees).
- Autoguiding should be ON.
- For each camera set the internal focus correctly and find the current expected telescope focus value. Go $\pm$ 150 telescope focus steps around the expected focus value in steps of 25 units.
- For each focus value take a good S/N image (without saturation) *without* the focus pyramid and one image *with* the focus pyramid.
- During the test dither the telescope about 10” a couple of times to allow for sky subtraction.

This test necessarily must be kept rather interactive for the time being. When the sequencer works it could probably be done in a script.

A script for reducing the data is not yet available.

7.3 Plate solution and optical distortion

The detailed procedure for the determination and correction of the optical distortion of each camera is to be looked further into.

7.4 Shutter accuracy

The shutter accuracy should be tested about once per year. Turn on the NOTCam calibration lamp in the dome (at the time of writing this is the bulb on the floor). Use the same instrument setup as for the detector QC (WF camera, J filter, etc.). Open mirror covers. Make sure that nobody enters the dome. Run the script **shutter.run**.

This script takes exposures with 13 different exposure times (10, 8, 6, 4, 2, 1.5, 1, 0.8, 0.6, 0.5, 0.4, 0.3, and 0.2 seconds), interspersed with 10 s exposures to monitor the lamp stability. For each exposure there is also a corresponding dark taken right before the exposure. In between each frame there is a **clear** command to clean the array. The whole script takes 18 minutes and produces 52 files.

For each exposure subtract the corresponding dark. Divide each of the 13 exposure time images by the most nearby 10 second exposure to correct for lamp variability. Use a central area on the array which is free of bad pixels, for instance [540:640,570:670], and make image statistics of this area. Plot the median value of each image versus the exposure time. This shows a linear relation (see Fig. 11). In order to enhance possible deviations from linearity, normalize this signal by dividing it by the exposure time. The data set might have spurious erroneous values (possibly due to lamp variability or jumps in the dark level) which should be excluded in the calculation of the shutter timing correction.

An IRAF script **shut_qc.cl** which does these steps is under construction.

7.5 Memory effects

The memory effect can be tested by taking an argon lamp exposure followed by several > 10 darks. This is convenient as you can follow the memory effect of different intensity levels in the same image. The best evaluation of the memory effect is made with a bright star which is dithered across the FOV. This lets one test the real effects of the memory effects in practice as sky exposures usually are background limited as opposed to darks.

A standard test is to be defined.

References

Abbott, T.M.C., Aspin, C., Sørensen, A.N., et al. 2000, *SWIR at the Nordic Optical Telescope: NOTCam*, Proc. SPIE Vol. 4008, 714-719

Atad, E., 1997, *NOTCam Optical Design*, http://www.not.iac.es/instruments/notcam/OpticalDesig

Cox, G. 1998, *Heat Load from the Internal NOTCam Motor Wires*, http://www.not.iac.es:/instruments/notcam/WireHeatLoad.ps

Cox, G. 2004, *Review of NOTCam Bearings*, http://www.not.iac.es:/instruments/notcam/bearings.pdf

Cutri, R.M., Skrutskie, M.F., Van Dyk, S., et al. 2003, *Explanatory Supplement to the 2MASS All Sky Data Release*, http://www.ipac.caltech.edu/2mass/releases/allsky/doc/explsup.html

Dye, S., Warren, S.J., Hambly, N.C., et al. *The UKIRT Infrared Deep Sky Survey Early Data Release* 2006, astro-ph/0603608

Fuensalida, J.J., Alonso, A. *Characterization of the atmospheric extinction in the near infrared at the Teide Observatory* 1998, New Astronomy Reviews 42, 543

Glass, Ian S. 1999, *Handbook of Infrared Astronomy*, Cambridge University Press

Hammersley, P. *Infrared quality of the Canarian skies* 1998, New Astronomy Reviews 42, 533

Hewett, P.C., Warren, S.J., Leggett, S.K., Hodgkin, S.T. *The UKIRT Infrared Deep Sky Survey ZYJHK Photometric System: Passbands and Synthetic Colours* 2006, MNRAS, in press

Hodapp, K.-W., Hora, J.L, Hall, D.N.B., et al. 1996, New Astronomy 1, p 177-196

Klougart, J. 2006, *NOTCam BIAS - the data acquisition software*, http://www.not.iac.es/instruments/notcam/notcamBIAS.html

Leggett, S.K., Currie, M.J., Varricatt, W.P., et al. *JHK Observations of Faint Standard Stars in the Mauna Kea Near-Infrared Photometric System* 2006, MNRAS, in press, astro-ph/0609461

Mackay, C.D. 1999, *The Reset Anomaly in HAWAII-1, 1024 x 1024 Arrays*, http://www.ast.cam.ac.uk/ optics/cirsi/documents/resetanomaly.html

McLean, Ian S. 1997, *Electronic Imaging in Astronomy, Detectors and Instrumentation*, John Wiley & Sons

Sørensen, A.N. 2000, *NOTCam: Vacuum and cryogenic characterization*, IJAF technical report # 6

Telting, John 2004, *Commissioning of the spectroscopic mode of NOTCam*, http://www.not.iac.es/instruments/notcam/spectroscopy/speccomm.html

A WF camera plate solution

The plate solution found with the task *ccmap* in IRAF using 85 stars common to a NOTCam 3.6' trimmed image of a young cluster and the 2MASS database is listed. Obtained for the H band filter with the Science Array in January 2006.

```
begin   85h_plsol.dat
        xrefmean        452.323294117647
        yrefmean        443.257529411765
        lngmean         101.2574972235294
        latmean         0.2225231764705882
        pixsystem       logical
        coosystem       j2000
        projection      tnx
        lngref          101.2574962897245
        latref          0.222523187016404
        lngunits        degrees
        latunits        degrees
        xpixref         452.6696027442571
        ypixref         444.9191166434474
        geometry        general
        function        polynomial
        xishift         -102.7829028153386
        etashift        -106.8972968053154
        xmag            0.2335897194112298
        ymag            0.2335109783424124
        xrotation       269.4017341291331
        yrotation       89.35800554206259
       wcsxirms        0.147095318576334
        wcsetarms       0.1420299005793626
        xirms           0.1470953185763343
        etarms          0.1420299005793626
        surface1        11
                        3.      3.
                        2.      2.
                        2.      2.
                        0.      0.
                        6.73    6.73
                        858.3899999999999       858.3899999999999
                        14.77   14.77
                        875.8500000000001       875.8500000000001
                        -102.7829028153386      -106.8972968053154
                        -0.002439027300844539   0.2335769855110791
                        0.2334963197770349      0.002616420648760438
        surface2        17
                        3.      3.
                        3.      3.
                        3.      3.
                        1.      1.
                        6.73    6.73
```

```
858.3899999999999        858.3899999999999
14.77   14.77
875.8500000000001        875.8500000000001
0.941019456840195        0.849091029299246
-0.007170434606740272   -0.001119557851804223
8.899180327925691E-6    -1.401635472211381E-6
-0.003818985325223676   -0.005688834226095727
2.178394719139697E-5     1.252925252443285E-5
-2.594079386562193E-8    7.609202787925185E-10
2.666398030738543E-6     5.337684218319608E-6
-9.535610454852559E-9   -1.146454080777119E-8
1.049348960677956E-11   -1.545930662062502E-12
```